Wake-field excitation in two- and three-component plasmas

David W. Aossey
Department of Electrical and Computer Engineering, The University of Iowa, Iowa City, Iowa 52242

James E. Williams, Hyun-Soo Kim, Jamie Cooney, and Yung-Chun Hsu
Department of Physics and Astronomy, The University of Iowa, Iowa City, Iowa 52242

Karl E. Lonngren
Department of Electrical and Computer Engineering and Department of Physics and Astronomy, The University of Iowa, Iowa City, Iowa 52242

(Received 13 October 1992)

Experiments on plasma wake fields are presented. Properties of wake fields in a two-component plasma are briefly reviewed and compared with the experiments of Nishida *et al.* [Phys. Rev. Lett. **66**, 2328 (1991)]. Characteristics of wake fields in a three-component plasma that consists of positive ions, negative ions, and electrons are then described. These wake fields are created following the injection of either positive or negative ions into a plasma. The relationship between ion-acoustic fast modes and the wake field are investigated and the excitation mechanism is discussed. Critical negative-ion concentrations and modulation effects are examined. The excitation of the wake fields is interpreted using a fluid model.

PACS number(s): 52.35.Mw, 52.75.Di

I. INTRODUCTION

A topic of current research in plasma physics is that of plasma wake-field phenomena. The impetus for this investigation is to establish techniques that will assist in the development of high-energy particle accelerators [1–3]. Plasma wake-field accelerators usually employ a carefully tailored burst of relativistic electrons that are injected into a plasma. A characterizing feature of the wake-field mechanism is that there is often a lengthy trail of relatively large amplitude nondispersive oscillations whose frequency is of the order of the electron plasma frequency that follow behind, or in the "wake" of, the initial set of density perturbations traveling through the plasma.

Recently, Nishida, Okazaki, Yugami, and Nagasawa have shown that many of the features that are unique to a wake field with relativistic electrons can also be observed with low-energy ion bunches injected into a plasma in a double plasma machine [4]. In these experiments, large amplitude nondispersive trailing oscillations were reported that had a frequency that was of the order of the ion plasma frequency. Since the time scales in these experiments were determined by the ions rather than the electrons, properties of an ion wake field could be easily elucidated. Appropriate scaling would make these results germane to the higher-frequency electron wake field. The tailoring of the injected ion beam demonstrated that rise and fall times and the amplitude of the applied voltage signals were critical factors in exciting large amplitude wake fields. The nondispersive oscillations that appear in wake fields that were observed in this experiment, and in the experiment that will be described below, differ from the small amplitude dispersive oscillations that are found in either linear ion-acoustic wave or ion-acoustic wave shock experiments [5].

In the present paper, we describe a series of experiments designed to unearth additional properties of the ion wake field. Our initial results complement the experiments of Nishida *et al.* [4] that were obtained in a two-component positive-ion–electron plasma. Experiments that were obtained in a three-component positive-ion–negative-ion–electron plasma are then described. The experimental results are summarized briefly as follows. In the two-component plasma, the optimal excitation of the wake field is related to an initial perturbation that depends on the amplitude and the rise and fall times of the excitation signal, as well as the density of the plasma. In the three-component plasma, we find that the wake-field excitation depends, in addition to these parameters, on additional parameters that represent the negative-ion concentration and the sign of the excitation voltage signal.

The experimental setup is described in Sec. II. Section III contains the experimental results and observations. A linearized wake-field model characterizing a three-component plasma is developed in Sec. IV. Concluding remarks are presented in Sec. V.

II. EXPERIMENTAL SETUP

The experiments were conducted in a large vacuum chamber that has been described elsewhere [6]. Two cubic multidipole magnetic cages ($40\times40\times40$ cm^3) were used to confine the plasma. The cages consisted of several rows of hollow rectangular tubes filled with small permanent magnets. The magnet pole faces in each row pointed in the same direction. The rows alternated in magnetic pole orientation, creating the magnetic barrier necessary to contain the plasmas. A fine mesh screen at a negative floating potential separated the cages. The

screen prevented electron flow between the cages.

The experimental plasmas were produced as follows. The base vacuum pressure was maintained beneath 10^{-6} Torr by continuous pumping. Argon was bled through a valve into the chamber and maintained at a neutral pressure of approximately 2.0×10^{-4} Torr. Ionizing electrons from the target and driver filaments were accelerated by bias voltages applied between the filaments and the respective anodes. Each cage was independently biased and supported a series of filaments that were independently heated. Nominal target and driver bias voltages were 80 and 60 V, respectively, and nominal target and driver filament currents were 24 and 20 A, respectively. In one experimental case described later, the driver bias voltage and filament current were switched off, resulting in a low-density plasma in the driver that had "leaked" from the target.

The difference of the plasma potentials between the two chambers could be controlled with a dc bias voltage. A periodic excitation voltage signal, typically of the order of 10 V and 1–2 kHz, was applied to one of the confinement cages resulting in a flow of ions from one cage to the other through the separation screen. The cage with the applied signal voltage is referred to as the driver, and the other cage where the measurements were made is referred to as the target.

To create the three-component positive-ion–negative-ion–electron plasma, sulfur hexafluoride (SF_6) was bled into the vacuum chamber through a separate valve until the electron saturation current indicated the desired negative-ion concentration. Several types of negative ions could be present in the plasma. SF_6 has a high affinity for electron capture at low energies. The formation of SF_6^- would predominate with the plasma electrons where $T_e\approx1$ eV. At higher energies, bombardment of SF_6 by the 80 eV primary electrons and lower energy scattered secondaries yields F^- from dissociative ionization. When this is the case the lighter and therefore faster F^- ions will determine the plasma response to small perturbations. We see evidence of the heavier SF_5^- and SF_6^- ions in bursts. No measurement was made of the relative abundances of the negative ions.

Typical two-component plasma numbers monitored with Langmuir probes in each chamber were a positive-ion density n_{+0} of $(2-5)\times10^8$ cm^{-3} and an electron temperature T_e of 1–3 eV. The ion temperature T_i was $T_i<T_e/10$. The negative-ion concentration ϵ was estimated by measuring the reduction in the electron saturation current [7]. We assume the introduction of SF_6 doesn't alter the positive-ion density and define the parameter ϵ to be

$$\epsilon=\frac{n_{-0}}{n_{+0}}=\frac{n_{+0}-(n_{+0}-n_{-0})}{n_{+0}}=1-\frac{I_{es}}{I_{es(0)}}\ , \qquad (1)$$

where I_{es} and $I_{es(0)}$ are the Langmuir probe saturation currents with and without SF_6, respectively [8]. The negative-ion density is expressed as n_{-0}.

The plasma signals of interest in this experiment were excited by controlling the flow of particles from the driver to the target. The driver anode excitation signals varied in shape and polarity and will be described on a case by case basis with regard to the particular experiment in question. Excitation signal repetition rate was maintained at less than 2 kHz in order to allow for plasma dynamic processes to fully develop and the plasma to equilibrate between excitation pulses.

All signals were detected with a 3-mm-diam spherical Langmuir probe that could be moved axially and azimuthally within the target volume. The separation grid was defined as $z=0$ with z increasing into the target chamber. The probe was biased positive with respect to the plasma potential in order to detect perturbations in the electron saturation current. The perturbations in the current were passed through a resistor to ground and the resulting voltage perturbations were displayed on a LeCroy digital oscilloscope that was triggered from the signal generator. An interactive data-acquisition routine was used to send and store the experimental data from the oscilloscope to a Macintosh computer via the general purpose interface bus. To avoid spurious results, all oscilloscope signals were a summed average of 100 wave form samples.

III. EXPERIMENTAL RESULTS

The experimental results contained in this paper will be presented in two parts. The first part consists exclusively of wake-field effects in a two-component plasma which confirm and expand on that which was reported by Nishida *et al.* [4]. In the second part, results of wake-field experiments in a three-component plasma are presented.

A. Wake-field effects in a two-component plasma

A series of four experiments were conducted under various plasma parameters, each with regard to a specific excitation signal or wave attributes. The four separate characteristics are as follows: (i) excitation voltage fall time, (ii) excitation voltage rise time, (iii) initial perturbation velocity, and (iv) amplitude decay of the wake field.

Figure 1 exhibits data for various values of excitation signal fall time when the detecting probe is fixed at 3 cm from the separation grid. Signal amplitude is measured with respect to the steady-state background electron density, $n_0=n_{+0}$. Figures 1(b)–1(f) show the plasma response to the corresponding excitation voltage shown in Fig. 1(a). In this experiment only, the driver filaments and bias voltage were switched off. An electrostatically coupled voltage perturbation follows the change of slope of the applied signal for $0\le t\le30$ μs. The oscillation signal that appears after $t\approx30$ μs will be called the "wake field" in the remainder of this paper. The amplitude decayed gradually in an undulatory manner as the fall time increased. Figure 2 is a summary of this dependence on fall time. These results are in substantial agreement with those reported by Nishida *et al.* [4].

Figure 3 shows traces for various values of the excitation signal rise time when the detecting probe is fixed at $z=15$ cm. Figures 3(b)–3(f) display the plasma response to the corresponding excitation voltages shown in Fig. 3(a). The rise times ranged from 5 to 100 μs for an excitation pulse that is significantly wider than that shown in Fig. 1. The detected signals indicate the presence of an initial burst of ions followed by an oscillation signal of

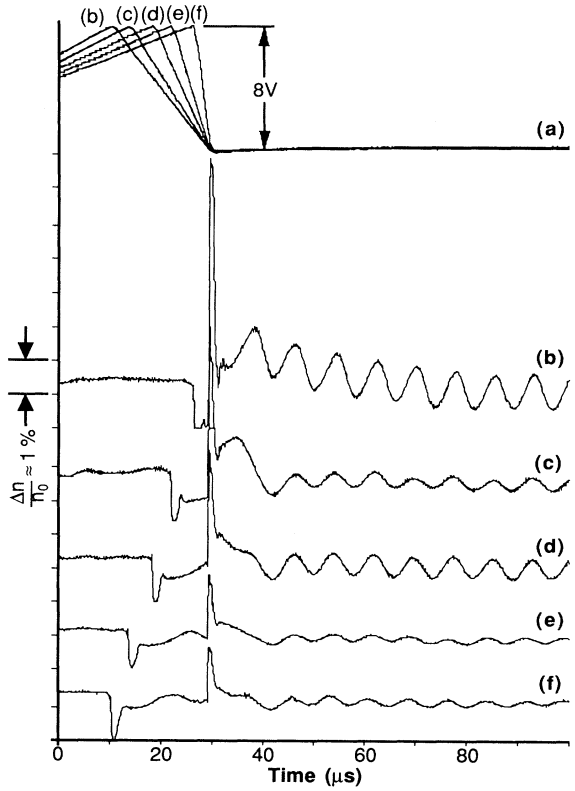

FIG. 1. Fall-time effects on positive-ion wake fields. (a) Excitation signals with fall times of 20, 16, 12, 8, and 4 μs. (b)–(f) Associated wake fields. The probe was at $z=3$ cm.

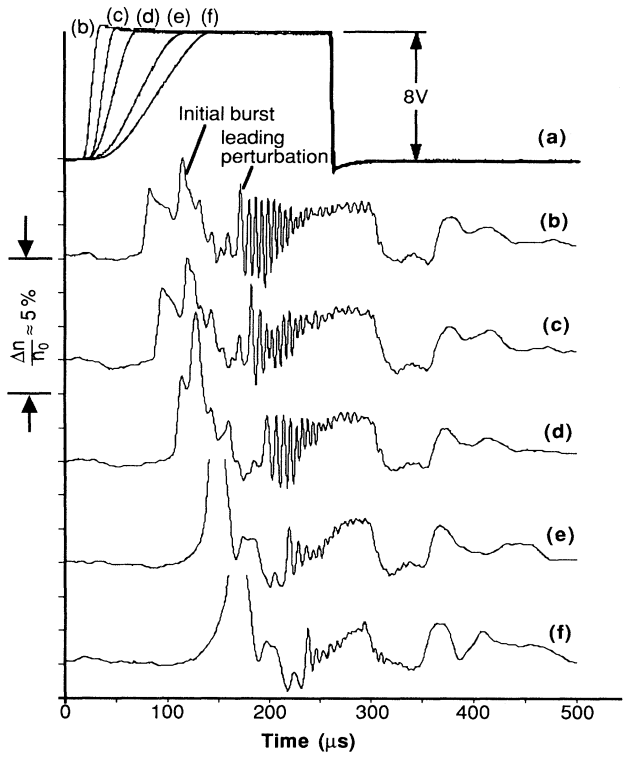

FIG. 3. Rise-time effects on positive-ion wake fields. (a) Excitation signals with rise times of 5, 15, 40, 65, and 100 μs. (b)–(f) Associated wake fields. The probe was at $z=15$ cm.

varying strengths. Associated with the wake field is a leading perturbation which is indicated in Fig. 3.

The period of the oscillating signal is approximately constant over the course of at least ten cycles. This indicates that it is nondispersive and allows us to differentiate it from the dispersing Airy function signal that trails an ion-acoustic shock, soliton, or linear wave [5]. The rise time, like fall time, seems to have no overall effect on the wake-field frequency. As the rise time increases, Fig. 3 reveals that the initial burst amplitude increases while the wake-field amplitude diminishes and eventually dissipates along with the amplitude of the leading perturbation. This leads us to hypothesize that the wake field is excited by the leading perturbation and not by the initial burst of ions as has been conjectured previously [4]. Subsequent results will show that this initial perturbation is ion acoustic in nature.

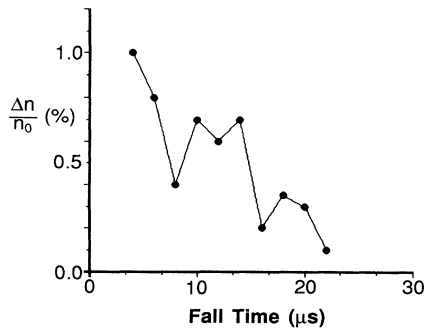

FIG. 2. Plot of amplitude vs excitation signal fall time.

The wake field in Fig. 3 appears to follow the rising edge of the excitation signal in contrast to the data shown in Fig. 1 and in the earlier experiment where it followed the trailing edge [4]. In fact, the oscillations are observed before the falling edge of the excitation pulse has occurred. This suggests that the critical parameter involved in the excitation of the ion wake field is the shape of the ion perturbation that is launched into the target by the excitation voltage. We have found in the past that this is the crucial property for soliton excitation in the laboratory using grids, solid metal plates, and double plasma machines [9]. This conjecture will be examined in detail below, in particular, when the details of the experiment using the three-component plasma are described.

The spatial evolution of the wake field in a two-component plasma is depicted in Fig. 4. Two features of the trailing oscillations are readily apparent. First, the oscillations appear to "propagate" away from the separation grid. Second, there appears to be an initial growth in amplitude, a maximum value, and a subsequent decay. The propagation of the density depression indicated by the arrow in Fig. 4 ($z=6$ cm) is plotted in Fig. 5(a) yielding a velocity of 1.1×10^5 cm/s. We interpret this depression as preceding the leading perturbation that ex-

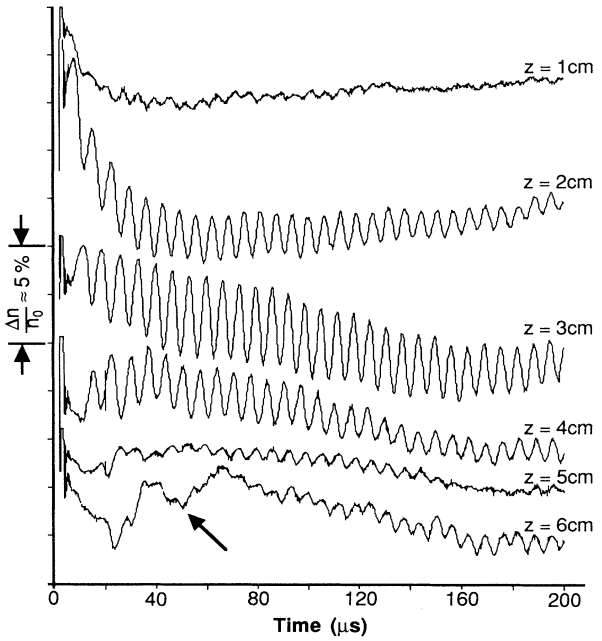

FIG. 4. Spatial evolution of a wake field. The arrow at $z=6$ cm indicates a density depression preceding the perturbation that excites the wake field.

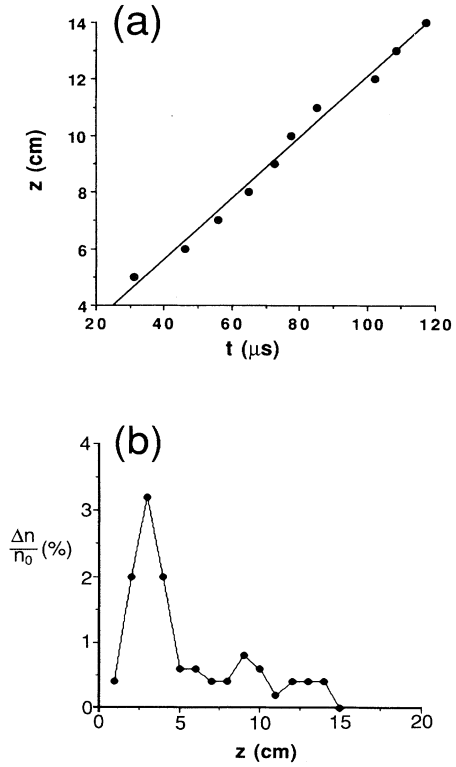

FIG. 5. Characteristics of the wake field in Fig. 4. (a) "Time-of-flight" plot for the density depression indicated in Fig. 4. The velocity is 1.1×10^5 cm/s. (b) Amplitude profile of peak-to-peak maxima.

cites the wake field. The spatial decay of the maximum peak-to-peak amplitude is plotted in Fig. 5(b). The peak field amplitude occurs at approximately $z=3$ cm under the given plasma conditions.

B. Wake-field effects in a three-component plasma

In this part, we present the results of various experiments involving the addition of negative ions to the two-component plasma and the resulting wake-field effects. With the addition of negative ions, we have introduced an additional degree of freedom. Positive *and* negative voltage signals applied to the driver chamber can inject positive and negative ions, respectively, into the target chamber. The individual ventures are summarized as follows: (i) The addition of SF_6 results in phase shifts and damping of an initially positive-ion–electron wake field; (ii) ion-acoustic fast modes are excited with both positive and negative excitation voltages as SF_6 is added; (iii) amplitude modulation of the wake field is observed with large positive excitation; and (iv) spatial damping and modulation of the wake field under negative excitation is observed. In all experiments, the portion of SF_6 is specified with the parameter ϵ that is defined in (1).

Figure 6 shows a series of oscilloscope traces taken with the probe fixed at $z=15$ cm as SF_6 was added to the chamber in discrete increments. The excitation signal was a *positive* 9-V step function with a rise time of 40 μs applied to the driver chamber. The first trace in Fig. 6 represents pure argon ($\epsilon=0$). An increase in negative-

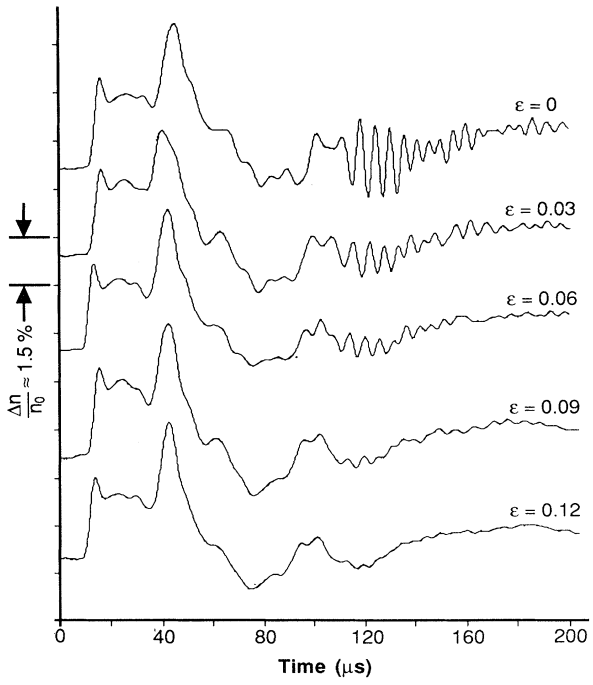

FIG. 6. Plasma wake fields for small negative-ion concentrations. The excitation signal was a *positive* 9-V step excitation with a rise time of 35 μs. Note phase shifting and damping associated with small increases in ϵ. The probe position was $z=15$ cm.

ion concentration causes a decrease in wake-field amplitude and a time shift of the field itself. The shift forward in time suggests that the wake-field excitation is related to the ion-acoustic fast mode in a three-component plasma [10]. The implication of this suggestion is that the perturbation exciting the wake field is a wave, specifically the leading perturbation per Fig. 3(b).

In order to observe in greater detail this possible fast mode excitation for a three-component ion wake field, the probe was set at $z=10$ cm and a *negative* excitation voltage was applied to the driver chamber. The resulting oscilloscope traces, corresponding to increasing values of ϵ, are shown in Fig. 7. At approximately $t=110$ μs in the first trace ($\epsilon=0$), a slight depression occurs which develops into the perturbation that leads the wake field. In subsequent traces taken with increasing values of ϵ, the velocity of this perturbation increases as indicated by its earlier occurrence in time. This is the first evidence of fast mode excitation. For $0.18<\epsilon<0.39$, we identify the train of oscillations trailing the leading perturbation as its dispersive components [5] since higher-frequency oscillations appear later in time. A further increase of ϵ yields a fully developed wake field that masks these oscillations. This is observed at approximately 60 μs for $\epsilon=0.49$. As with the wake field previously encountered, Fig. 7 shows that the field is not fully established until the leading perturbation develops into a signal of relatively large amplitude.

Figure 8(a) shows the ratio of the velocity of the leading perturbation in Fig. 7 to the ion-acoustic speed (its speed when $\epsilon=0$). The excitation signal ends at $t_0=40$ μs in Fig. 7. The velocity is then just $v_1=10\ \text{cm}/(t-t_0)$. The greater speed of this perturbation with increasing ϵ follows the increase in fast mode velocity in a three-component plasma. This again indicates that the excitation mechanism is a wave. We note an anomalous jump in the perturbation speed at $\epsilon\approx 0.3$.

The pulses that appear in Fig. 7 at $t\approx 52$ μs and at $t\approx 60$ μs remain stationary in time. We identify them as particle bursts with $t_{\text{burst}}=12$ μs and $t_{\text{burst}}=20$ μs. Their velocities approximately satisfy the relation

$$t_{\text{burst}}=\frac{z}{v_{\text{burst}}}=\frac{z}{\sqrt{2|e\phi|/M}}\ , \tag{2}$$

where z is the probe position of 10 cm, M is the particle mass (Ar or SF_6, respectively), and ϕ is the applied signal voltage of -8 V. Figure 8(b) shows that, as ϵ increases, the amplitude of the earlier Ar^+ burst shrinks while that of the later SF_6^- burst increases. At $\epsilon\approx 0.3$, the growth and decay rates of these bursts change anomalously. This corresponds with the appearance of the wake field. The

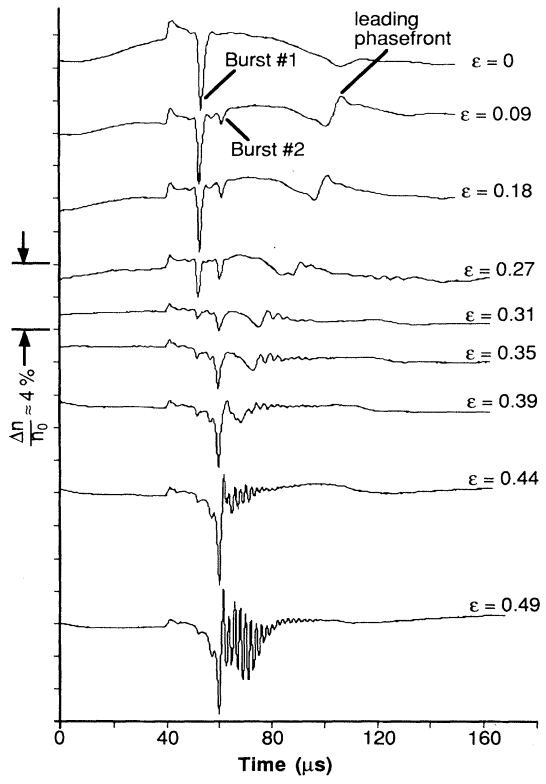

FIG. 7. Excitation of ion-acoustic perturbations and subsequent wake fields in a negative-ion plasma. The excitation signal was a *negative* 8-V step function with a fall time of 30 μs. The probe was at $z=10$ cm. The excitation signal ends at $t_0=40$ μs.

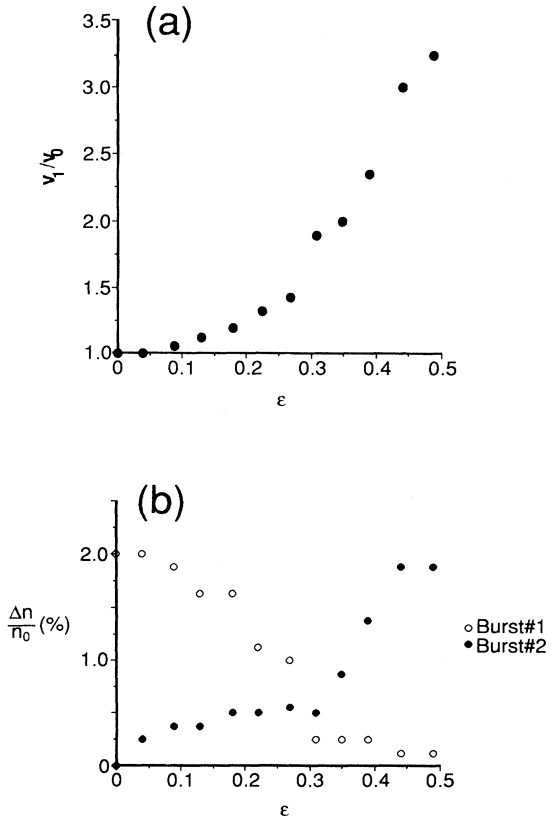

FIG. 8. Characteristics of the wake fields in Fig. 7. (a) Velocity of the leading perturbation vs ϵ. (b) Amplitude profile for the two particle bursts identified in Fig. 7. Both figures exhibit anomalous behavior at $\epsilon\approx 0.3$.

measured amplitude of the Ar^+ burst is considerably smaller than that for the SF_6^- burst at greater negative-ion concentrations.

For the experimental results presented thus far in this section, it was observed that a *negative* excitation voltage applied to a three-component plasma results in plasma wake fields at sufficient concentrations of SF_6. At higher negative-ion concentration (i.e., increasing ϵ), the generation of a large amplitude wake field in three-component plasmas with *positive* excitation voltage was also observed. The wake fields excited in this manner possessed slightly different properties than for the previous case of negative excitation, namely with regard to pronounced amplitude modulation effects for the positively excited wake field.

Figures 9(a) and 9(b) show a series of oscilloscope traces resulting from a +16 V ramp potential with a rise time of 50 μs applied to the driver anode. The time scales are different for each figure but the probe position in both cases was fixed at $z=10$ cm. The traces show the dependence of the wake-field amplitude on negative-ion concentration. Initially, a compressive ion burst appears as expected and then begins to decay with increasing ϵ. At $\epsilon \approx 0.4$, small dispersive oscillations appear. At $\epsilon \approx 0.6$ a fully developed nondispersive wake field is established. The figures indicate an amplitude modulation or phase mixing that was not apparent in the experiments employing a negative excitation.

A maximum amplitude $\Delta n/n_0$ of approximately 14% was observed for the wake field in Fig. 9(a). The plasma potential in Fig. 9(b) was slightly smaller than that for Fig. 9(a) and resulted in a maximum wake-field amplitude $\Delta n/n_0$ of approximately 20%. Ion wake fields are a low-density phenomenon that we observed when $n_{+0} < 5\times 10^8/\text{cm}^{-3}$. The largest wake-field amplitudes were found for low values of n_{+0}. In a negative-ion plasma the wake-field amplitude can also increase due to the replacement of electrons with negative ions. A plasma with n_{+0} positive ions and ϵn_{+0} negative ions has $n_0=(1-\epsilon)n_{+0}$ electrons. Then $\Delta n/n_0=\Delta n/(1-\epsilon)n_{+0}$ and the amplitude of a perturbation where Δn is a constant will scale as $1/(1-\epsilon)$. It thus follows that a negative-ion plasma provides an easy method to achieve large wake-field amplitudes. The relationship between maximum amplitude and densities—n_{+0} and n_0—appears to be an inverse one.

The spatial evolution of the wake field in a three-component plasma excited by a −10 V step of duration 200 μs with a fall time of 100 μs is shown in Fig. 10. The negative-ion concentration is approximately 25%. The field has the largest amplitude at $z=13$ cm. The amplitude has decayed to a negligible value at $z=22$ cm.

Two features of the wake-field oscillations are readily apparent as they also were in Figs. 4 and 5. First, the oscillations appear to "propagate" away from the separation grid. Second, there appears to be an initial growth in amplitude, a maximum value, and a subsequent decay of the oscillations. The "trajectories" of the first three cycles of the wake-field oscillations in Fig. 10 are plotted in Fig. 11(a). From this figure their "velocities" are determined to be $\approx 2.8\times 10^5$ cm/s. This is a greater value than that obtained for the wake fields in pure argon of Fig. 5(a), and again supports the hypothesis that the excitation occurs at the fast mode velocity for a three-component plasma.

Figure 11(b) is a plot of the spatial dependence of the amplitudes of the modulating envelopes observed in Fig. 10. The amplitude of the initial envelope (#1) decays at a faster rate than that of the succeeding envelope (#2). The existence of these envelopes is evidence that amplitude modulation effects are present for negative-going ex-

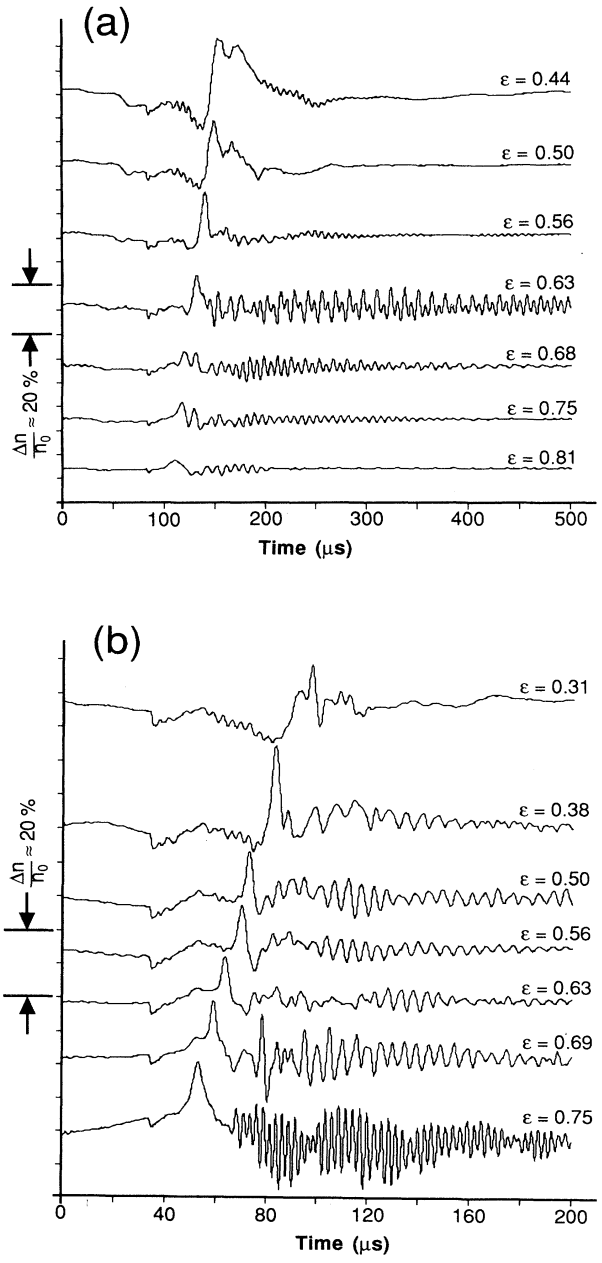

FIG. 9. Wake-field excitation at $z=10$ cm from a *positive* 16-V step for varying negative-ion concentrations. The plasma potential in (b) is slightly smaller than that of (a).

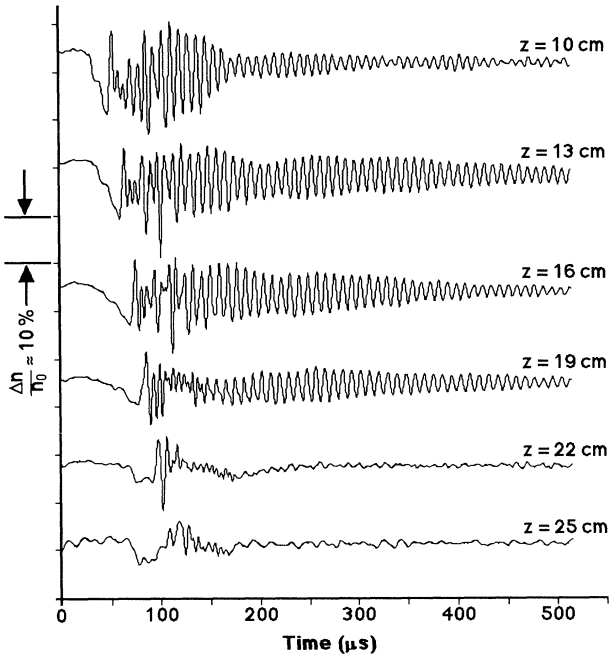

FIG. 10. Spatial evolution of a wake field in a negative-ion plasma. The excitation signal was a *negative* 10 V step function of 200-μs duration with a 100-μs fall time. The negative-ion concentration ϵ was $\approx 25\%$.

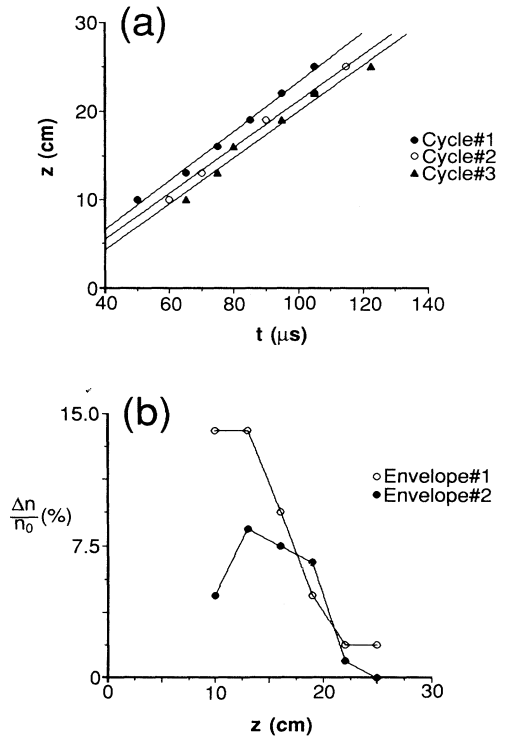

FIG. 11. Characteristics of the wake field in Fig. 10. (a) "Time-of-flight" plot for the leading three cycles. The velocities are approximately 2.8×10^5 cm/s. (b) Amplitude profile of the modulating envelopes.

citation as well as for positive excitation, an effect that was not initially observed in the earlier experimental observations involving negative excitation in the three-component plasma.

IV. INTERPRETATION

Wake fields in a pure electron plasma have been theoretically investigated using a simple linearized model developed by Ruth *et al.* [2]. The analysis of wake-field phenomena in positive- and negative-ion plasmas is more complicated due to the coupling between various particles and to the nonlinear effects that govern the dynamics of the field amplitude in space and time. For a multicomponent plasma, however, a nonlinear analysis in closed form becomes unwieldy. It is possible, nonetheless, to assess various wake-field effects in a two- and three-component plasma using a strictly linear model. The model we have chosen successfully predicts the sinusoidal behavior of the wake fields, the frequency of oscillation, and provides a criterion for wake-field excitation. We extend the low amplitude one-dimensional model proposed by Ruth *et al.* [2] to wake fields to a three-component cold ion plasma with n_{+0} positive ions, $n_{-0}=\epsilon n_{+0}$ negative ions, and $n_{e0}=(1-\epsilon)n_{+0}$ Boltzmann electrons. This is a good approximation for a discharge device where $T_i \ll T_e$.

The density perturbation of Boltzmann electrons n_e is expressed as

$$n_e = n_{e0}\exp\left[\frac{e\phi}{k_B T_e}\right],$$

where e is the electron charge, ϕ is the potential, k_B is Boltzmann's constant, and T_e is the electron temperature. Expanding the exponential and retaining the first-order term results in the first-order electron perturbation n_{e1},

$$n_{e1} = n_{e0}\left[\frac{e\phi}{k_B T_e}\right], \tag{3}$$

from which we obtain

$$\nabla n_{e1} = \frac{n_{e0}e}{k_B T_e}\nabla\phi = -\frac{n_{e0}e}{k_B T_e}\mathbf{E}, \tag{4}$$

where $\mathbf{E}$ is the first-order electric field.

The starting point for the ions is the unmagnetized fluid equations,

$$\frac{\partial n}{\partial t} + \nabla\cdot(n\mathbf{v}) = 0 \tag{5}$$

and

$$\frac{\partial \mathbf{v}}{\partial t} + (\mathbf{v}\cdot\nabla)\mathbf{v} = \frac{e}{m}\mathbf{E}. \tag{6}$$

Expanding these in a perturbation series and linearizing leads to the following set of ion equations for the positive ions (+) and the negative ions (−):

$$\frac{\partial n_{+1}}{\partial t}+n_{+0}\nabla\cdot\mathbf{v}_{+}=0$$
$$\frac{\partial n_{-1}}{\partial t}+n_{-0}\nabla\cdot\mathbf{v}_{-}=0 \tag{7}$$

and

$$m_{+}\frac{\partial \mathbf{v}_{+}}{\partial t}=e\mathbf{E}$$
$$m_{-}\frac{\partial \mathbf{v}_{-}}{\partial t}=-e\mathbf{E} \tag{8}$$

where m is the ion mass and $\mathbf{v}$ is the ion velocity. Differentiating (7) with respect to time and substituting (4) and (8) into it yield

$$\frac{\partial^2 n_{+1}}{\partial t^2}+n_{+0}\nabla\cdot\frac{\partial \mathbf{v}_{+}}{\partial t}=\frac{\partial^2 n_{+1}}{\partial t^2}+\nabla\cdot\left[-\frac{k_B T_e}{m_{+}}\frac{n_{+0}}{n_{e0}}\nabla n_{e1}\right]=0$$
$$\frac{\partial^2 n_{-1}}{\partial t^2}+n_{-0}\nabla\cdot\frac{\partial \mathbf{v}_{-}}{\partial t}=\frac{\partial^2 n_{-1}}{\partial t^2}+\nabla\cdot\left[\frac{k_B T_e}{m_{-}}\frac{n_{-0}}{n_{e0}}\nabla n_{e1}\right]=0\ . \tag{9}$$

Equations (4) and (9) constitute the dynamic representation of the three species of particles: electrons, positive ions, and negative ions.

The electron-density perturbation couples to the ion perturbations through Poisson's equation,

$$\nabla\cdot\mathbf{E}=\frac{e}{\epsilon_0}(n_{+1}-n_{-1}-n_{e1}+n_{ex})\ . \tag{10}$$

When the electric field is expressed by the electron-density perturbation in (4) we have in one dimension,

$$\frac{\partial^2 n_{e1}}{\partial z^2}=-\frac{n_{e0}e^2}{k_B T_e\epsilon_0}(n_{+1}-n_{-1}-n_{e1}+n_{ex})\ . \tag{11}$$

In this expression, we have assumed charge neutrality to lowest order. An additional charge perturbation n_{ex} represents a source in the next order. This source is a δ-function excitation perturbation,

$$n_{ex}\equiv\sigma\delta(z-v_{ex}t)\ , \tag{12}$$

where σ is a surface charge density, z is the spatial variable, and v_{ex} is the velocity of the perturbation. Transforming (11) into the frame of the excitation signal via the substitution $y=v_{ex}t-z$ leads to the following ordinary differential equation:

$$\frac{d^2 n_{e1}}{dy^2}=-\frac{n_{e0}e^2}{k_B T_e\epsilon_0}(n_{+1}-n_{-1}-n_{e1})-\frac{n_{e0}e^2}{k_B T_e\epsilon_0}\sigma\delta(y)\ . \tag{13}$$

An integration about this signal ($-0<y<+0$) yields

$$\left.\frac{dn_{e1}}{dy}\right|_{-0}^{+0}=-\frac{n_{e0}e^2}{k_B T_e\epsilon_0}\sigma\ . \tag{14}$$

The first-order perturbations n_{e1}, n_{+1}, and n_{-1} are nonexistent for $y<0$, the region of quiescent plasma [2]. We assume the perturbation has the form

$$n_{e1}=\xi_e\sin\Xi y \tag{15}$$

for $y>0$. The coefficient ξ_e and the term Ξ are found from (14) to satisfy the condition

$$\xi_e\Xi=-\frac{n_{e0}e^2}{k_B T_e\epsilon_0}\sigma\ . \tag{16}$$

The solution for the electron perturbation is

$$n_{e1}=-\frac{n_{e0}e^2\sigma}{k_B T_e\epsilon_0\Xi}\sin[\Xi(v_{ex}t-z)]\ . \tag{17}$$

Substitution of (17) into (9) gives

$$\frac{\partial^2 n_{+1}}{\partial t^2}-\frac{n_{+0}e^2\Xi\sigma}{m_{+}\epsilon_0}\sin[\Xi(v_{ex}t-z)]=0\ . \tag{18}$$

The positive-ion perturbation is then given by

$$n_{+1}=-\frac{n_{+0}e^2\sigma}{m_{+}\epsilon_0\Xi v_{ex}^2}\sin\Xi y\ . \tag{19}$$

Analogously the negative-ion perturbation is found to be

$$n_{-1}=\frac{n_{-0}e^2\sigma}{m_{-}\epsilon_0\Xi v_{ex}^2}\sin\Xi y\ . \tag{20}$$

This is out of phase with n_{e1} and n_{+1} which oscillate in phase. Equations (17), (19), and (20) determine the density perturbations of the plasma components.

The constant Ξ is determined from Poisson's equation (13) for the region of excited plasma, i.e., $y>0$ where $\delta(y)=0$,

$$n_{+1}-n_{-1}=n_{e1}-\frac{k_B T_e\epsilon_0}{n_{e0}e^2}\frac{d^2 n_{e1}}{dy^2}\ . \tag{21}$$

Substitution of the appropriate densities gives

$$\Xi=\frac{\Omega_{p+}}{v_{ex}}\sqrt{1-(1-\epsilon)\mathcal{R}+\epsilon(m_{+}/m_{-})}\ , \tag{22}$$

with

$$\mathcal{R}=\frac{m_{+}v_{ex}^2}{k_B T_e}=\frac{v_{ex}^2}{c_{s0}^2}\ ,\quad \Omega_{p+}=\left[\frac{n_{+0}e^2}{m_{+}\epsilon_0}\right]^{1/2} \tag{23}$$

and c_{s0}, the ion-acoustic velocity in a two-component plasma. A frequency ω can be defined so that $\sin\Xi y=\sin\omega(t-z/v_{ex})$,

$$\omega=\Omega_{p+}\sqrt{1-(1-\epsilon)\mathcal{R}+\epsilon(m_{+}/m_{-})}\ . \tag{24}$$

In a multicomponent plasma with several negative-ion species, we have found that the lightest negative ions dominate the propagation characteristics of waves since they respond with a greater velocity to an applied pertur-

bation. For the purpose of analyzing the wake field, the plasma can be considered to consist of electrons, Ar^+ ions, and F^- ions with $m_+/m_-=2.1$. From measured values for the wake field in Fig. 10 ($c_{s0}=2\times10^5$ cm/s, $v_{ex}=2.8\times10^5$ cm/s, $\mathcal{R}=1.96$, $\epsilon=0.25$, and $n_{+0}=2\times10^8$ cm^3), we calculate an oscillation period $T=2\pi/\omega=9.0$ μs. This agrees closely with the measured T of 8.7 μs. The same values for c_{s0} and n_{+0} were found when observing the wake field of the two-component plasma ($\epsilon=0$) of Fig. 5. With $v_{ex}=1.1\times10^5$ cm/s, T is calculated to be 2.5 μs. This is of the same order as the measured $T=6.5$ μs. Our interpretation seems to be an adequate description of a three-component wake field but needs further refinement to explain the two-component plasma wake field.

V. CONCLUSIONS

A series of experiments describing plasma wake-field effects in both a positive-ion–electron plasma, and a positive-ion–negative-ion–electron plasma are presented. In the first case, results in agreement with Nishida *et al.* [4] are obtained and extended. A nondispersive wake field excited by an ion-acoustic perturbation was observed. In the second case, these excitation perturbations occurred at the fast mode velocity. These results are in substantial agreement with a theoretical linearized fluid model that is developed and described in this investigation. When the positive-ion density was decreased and the negative-ion concentration increased, large amplitude wake fields were attained. Amplitude modulation of wake fields excited by both positive-going and negative-going potentials were seen. These nonlinear effects await further theoretical interpretation.

ACKNOWLEDGMENTS

The authors would like to express their thanks to Paul Hansen for discussions. We also wish to thank Al Scheller for constructing most of the experimental apparatus. This work was supported in part by the National Science Foundation Grant No. ECS 90-06921.

[1] P. Chen, J. M. Dawson, R. W. Huff, and T. Katsouleas, Phys. Rev. Lett. **54**, 693 (1985); J. Dawson, Sci. Amer. **260**, 54 (1989).
[2] R. D. Ruth, A. W. Chao, P. L. Morton, and P. B. Wilson, Part. Accel. **17**, 171 (1985).
[3] M. E. Jones and R. Keinigs, IEEE Trans. Plasma Sci. **PS-15**, 203 (1987).
[4] Y. Nishida, T. Okazaki, N. Yugami, and T. Nagasawa, Phys. Rev. Lett. **66**, 2328 (1991).
[5] R. J. Taylor, D. Baker, and H. Ikezi, Phys. Rev. Lett. **24**, 206 (1970); C. Chan, M. Khazei, K. E. Lonngren, and N. Hershkowitz, Phys. Fluids **24**, 1452 (1981); H. Ikezi, Y. Kiwamoto, K. E. Lonngren, C. M. Burde, and H. C. S. Hsuan, Plasma Phys. **15**, 1141 (1973).
[6] J. M. Bulson, K. Huynh, E. F. Gabl, and K. E. Lonngren, J. Appl. Phys. **55**, 693 (1984).
[7] H. Amemiya, J. Phys. D **23**, 999 (1990).
[8] G. O. Ludwig, J. L. Ferreira, and Y. Nakamura, Phys. Rev. Lett. **52**, 275 (1984).
[9] E. K. Tsikis, S. Raychaudhuri, E. F. Gabl, and K. E. Lonngren, Plasma Phys. Cont. Fus. **27**, 419 (1985).
[10] N. D'Angelo, S. v. Goeler, and T. Ohe, Phys. Fluids **3**, 1605 (1966).